Protective Relay Synchrophasor Measurements During Fault Conditions

Armando Guzmán, Satish Samineni, and Mike Bryson
Schweitzer Engineering Laboratories, Inc.

Published in
SEL *Journal of Reliable Power*, Volume 2, Number 2, May 2011

Previously presented at the
5th Annual Clemson University Power Systems Conference, March 2006,
and 32nd Annual Western Protective Relay Conference, October 2005

Original edition released July 2005

Protective Relay Synchrophasor Measurements During Fault Conditions

Armando Guzmán, Satish Samineni, and Mike Bryson, *Schweitzer Engineering Laboratories, Inc.*

***Abstract*—This paper describes details of the signal processing techniques that a protective relay uses to provide both synchronized phasor measurements and line distance protection. The paper also presents a comprehensive system model of normal and faulted power system operating conditions. Finally, the paper provides power system model test results that demonstrate the ability of the described protective relay to provide synchrophasor measurements during both normal and faulted conditions.**

I. Introduction

Traditionally, dedicated phasor measurement units (PMUs) have provided synchronized phasor measurements. These PMUs are not in widespread use because they are relatively expensive and are only used on critical systems. Now, through use of proper signal processing techniques, a modern protective relay (referenced throughout this paper as a phasor measurement and control unit, or PMCU) can provide synchronized phasor measurements in addition to line distance protection [1]. This paper presents the techniques by which the PMCU achieves this dual functionality. To determine how well the PMCU performs these functions, we created a system model that includes a GPS clock receiver, a Real Time Digital Simulator (RTDS®), several PMCUs, a synchrophasor processor, and visualization software applications such as EPG RTDMS and BPA PDC StreamReader. We modeled two power systems: a three-source model and a simple two-source model. The power system models included machine and system control dynamics. In the three-source model, relay protection functions cleared the applied faults. We retrieved the calculated impedances and synchronized phasor measurements in this system. In the two-source model, we cleared faults manually to verify that the measured critical clearing time matched theoretical values. In both systems, we compared retrieved values with RTDS-calculated phasor data. Test results show that these relays provide reliable synchronized phasor measurements, that they are a more economical option than traditional PMU technology, and that they represent a feasible option for making synchronized phasor measurements available across the power system.

II. Sampling and Signal Processing

The PMCUs depicted in Fig. 1 are multiple power system application devices. To provide synchronized phasor measurements, these devices must have accurate time information. GPS satellite-synchronized clocks with microsecond accuracy provide this information through demodulated IRIG-B signals to the PMCUs. Proper time synchronization allows PMCUs at various power system locations to obtain time-synchronous samples of voltages and currents for use in calculating voltage and current time-synchronized phasors.

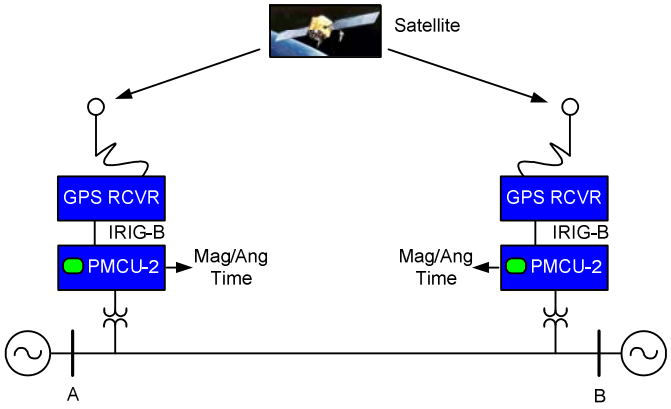

Fig. 1. PMCUs require GPS satellite-synchronized clocks with microsecond accuracy to provide synchronized phasor measurements.

Fig. 2 shows a data acquisition and data processing system suitable for multiple applications (distance protection, synchronized phasor measurement applications, and oscillography). Synchronized phasor measurement applications require sampling referenced to an absolute time reference, and line distance protection applications require sampling at multiples of the power system operating frequency.

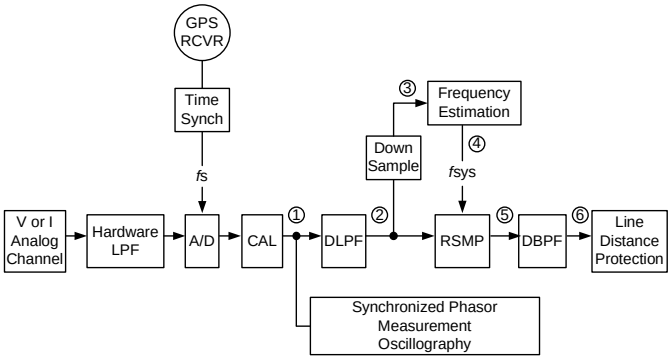

Fig. 2. PMCU sampling with an absolute time reference for synchronized phasor measurement applications and resampling at multiples of the power system operating frequency for line distance protection applications.

For synchronized phasor measurement applications, a PMCU acquires power system data at fixed time intervals; the sampling frequency (f_S) depends on an external clock signal (GPS clock receiver) that provides the absolute time reference. After the A/D converter acquires the data, data calibration

compensates for hardware data acquisition errors. The calibrated data ① are available at a high sampling rate (e.g., 8 kSPS) and are suitable for synchronized phasor measurement and oscillography applications. Data obtained at the high sampling rate pass through a digital low-pass filter (DLPF) before downsampling and resampling. The downsampler yields data at a lower rate ③ for frequency estimation. One of the inputs to the resampler (RSMP) is the filtered signal ②. The second input to the resampler is the power system operating frequency (f_{SYS}) ④. The resampler yields data ⑤ at a rate that is a multiple of the operating frequency (f_{SYS}) (e.g., 32 • f_{SYS}). The resampled data pass through a digital band-pass filter (DBPF). The DBPF has fixed coefficients that are not related to the power system operating frequency (f_{SYS}). The filtered data ⑥ are then ready for distance protection applications [2].

III. Synchronized Phasor Measurements

The PMCU synchronized phasor measurements use data at a fixed sampling frequency for angle and magnitude calculations (see Fig. 2). Fixed sampling frequency prevents local frequency measurement errors. Consider a sinusoidal voltage waveform, v(t) = A • cos(ω • t + φ), and assume multiplication of this waveform by a time-synchronized unit phasor, according to the following equation [3] [4]:

$$v_e(t) = A \bullet \cos\left(\omega \bullet t + \varphi\right) e^{-j\,\omega_0 t} \tag{1}$$

Which can be otherwise expressed as (2):

$$v_e(t) = A\left[\frac{e^{j(\omega t+\varphi)} + e^{-j(\omega t+\varphi)}}{2}\right] e^{-j\,\omega_0 t} \tag{2}$$

or as (3):

$$v_e(t) = \frac{A}{2}\left[e^{j\left[(\omega-\omega_0)\,t+\varphi\right]} + e^{-j\left[(\omega+\omega_0)\,t+\varphi\right]}\right] \tag{3}$$

Equation (3) has two terms: the low-frequency term that corresponds to the $(\omega - \omega_0)$ frequency,

$$v_{e\_LF}(t) = \frac{A}{2} \bullet e^{j\left[(\omega-\omega_0)\,t+\varphi\right]} \tag{4}$$

and the near double frequency term that corresponds to the $(\omega + \omega_0)$ frequency,

$$v_{e\_DF}(t) = \frac{A}{2} \bullet e^{-j\left[(\omega+\omega_0)\,t+\varphi\right]}$$

We are interested in the low-frequency term as a source for the synchronized phasor magnitude and phase. If we filter out the signal with the $(\omega + \omega_0)$ frequency, we obtain the low-frequency component (4). The computed signal has the input signal amplitude divided by two. After proper scaling, the computed signal v_{e_LF} can be represented in phasor form as follows:

$$\bar{V} = \frac{A}{\sqrt{2}} \angle \beta(t) \tag{5}$$

Where $\beta(t) = (\omega - \omega_0)\,t + \varphi$

The digital system Fig. 3 illustrates is equivalent to the procedure this paper describes for calculating the phasor. The input voltage signal passes through a traditional anti-aliasing low-pass filter (LPF). This filter has a cut-off frequency of 250 Hz. The PMCU decimates this 8 kHz filtered input voltage signal by 8 and then processes the resulting signal at 1 kHz. Fig. 3 also includes two LPFs with cutoff frequencies at 15 Hz and at least 20 dB attenuation for harmonics and interharmonics, providing 60 phasor measurements per second without aliasing problems. Fig. 4 shows the total filtering frequency response of the synchronized phasor measurement magnitude.

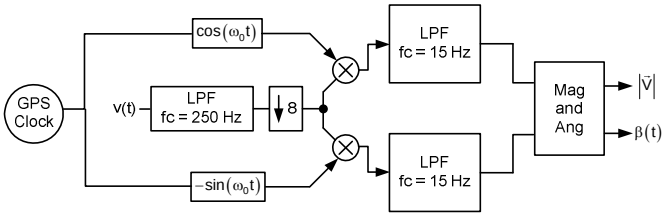

Fig. 3. A system to obtain phase and amplitude of the input signal using correlation.

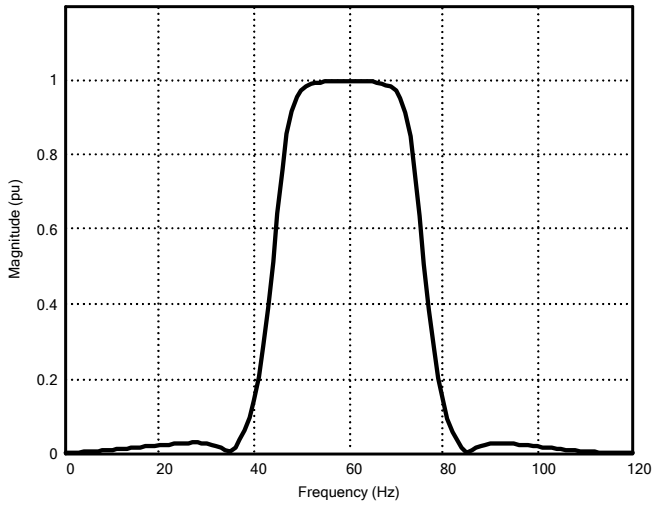

Fig. 4. Total filtering frequency response of the synchronized phasor measurement magnitude.

IV. Performance of Synchrophasor Measurements During Fault Conditions

A. Visualization and Dynamic Performance of Synchrophasor Measurements During Fault Conditions

Fig. 5 shows the power system model, synchrophasor data acquisition system, and visualization applications to analyze the performance of PMCU synchrophasor measurements during fault conditions. The power system was modeled in an RTDS. Four PMCUs measure voltages and currents at four system locations in the RTDS power system model. The breaker status and the trip signals are exchanged among the RTDS and PMCUs through input/output (I/O) boards, making the setup a real-time closed loop controlled power system. A GPS clock receiver provides a demodulated IRIG-B signal to the PMCUs for time synchronization. The PMCUs send synchrophasor data in IEEE C37.118 format at 60 messages

per second. A synchrophasor data processor collects and correlates the PMCU synchrophasor data. The synchrophasor data processor outputs correlated synchrophasor data according to IEEE C37.118 and BPA PDC Stream Format at 60 messages per second. Synchrophasor data processor and server software, EPG RTDMS software, and BPA PDC StreamReader software read and display correlated data to provide visualization of power system dynamics.

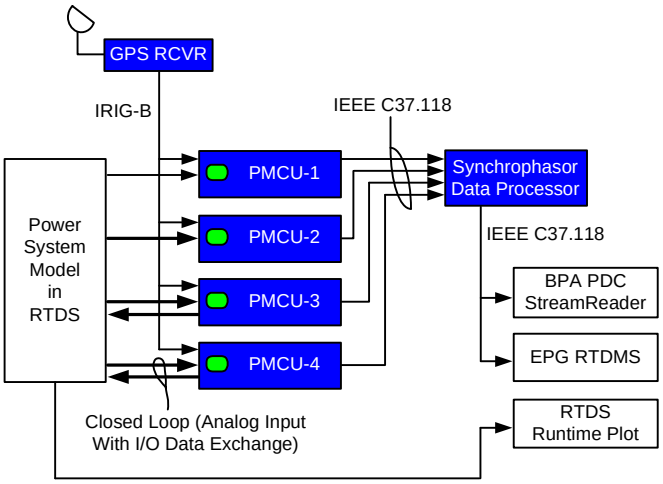

Fig. 5. Power system model, synchrophasor data acquisition, and visualization system.

1) Three-Source Power System Model

The RTDS power system model consists of three 400 MVA, 20 kV generators (G1, G2 and G3) with 20 kV/230 kV step-up transformers, four buses (1, 2, 3, and 4) with transmission lines (L1, L2, L3, and L4), and a dynamic load (LOAD), as shown in Fig. 6. PMCU-1, -2, -3, and -4 measure voltages at Buses 1, 2, 3, and 4; measure currents on lines L1, L2, and L3; then synchronize and send synchrophasor data to the synchrophasor data processor. PMCU-3 and PMCU-4 protect transmission line L3. PMCU-4 controls the load shedding at Bus 4 when transmission line L3 trips.

The generator models include generator dynamics, excitation systems, and hydroturbine governors. Table I in Appendix A lists data common to these models. The RTDS provides voltages and currents in real time and provides accurate representation of a real power system. The generators are scaled down 400-MVA-based models given in [5]. The 230 kV transmission lines L1, L2, L3, and L4 are each 200 km long and have the same line characteristic as that in Table I of Appendix A. The load is a constant P and Q load if the applied voltage is above 0.8 pu and constant impedance load if applied voltage is below 0.8 pu.

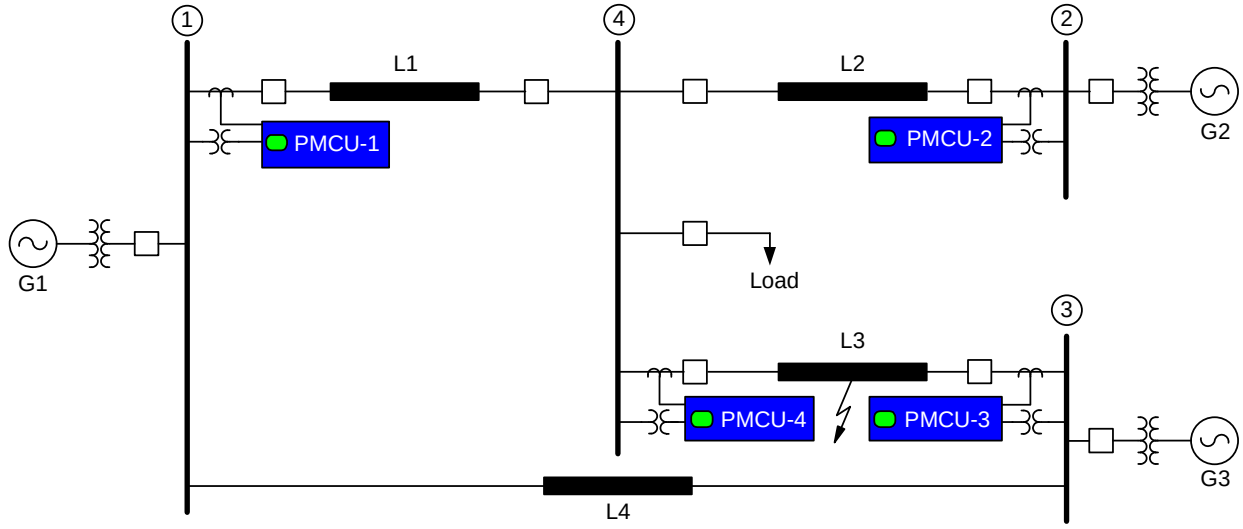

Fig. 6. Three-source RTDS power system model with four PMCUs for synchrophasor measurement and protection.

2) Visualization

During steady-state conditions, the three generators share load equally (148 MW each), and there is no real power flow on line L4. The phase angle (positive-sequence voltage synchrophasor) difference between Buses 1 and 2, Buses 2 and 3, and Buses 3 and 1 is almost zero. A three-phase fault occurs at 50 percent of line L3. PMCU-3 and PMCU-4 instantaneously trip line L3 within 4 cycles, based on Zone 1 distance protection. Generators G1 and G3 begin oscillating against Generator G2, and the system starts to become unstable because of these increasing oscillations. After 6 seconds, PMCU-4 sheds a third of the load at Bus 4, and the system becomes stable as the oscillations dampen out.

Fig. 7 shows the RTDS event capture of the power system dynamics. The first graph shows δ_{14}, the phase angle difference between Bus 1 and Bus 4. The second graph shows the frequencies measured at Bus 1, Bus 2, and Bus 3. The graphs labeled 3PT-3 and 3PT-4 show the trip signals PMCU-3 and PMCU-4 issued for clearing the three-phase fault on line L3. The graphs labeled 52AA1-3 and 52AA1-4 indicate breaker status at Bus 3 and Bus 4 on line L3. LD is the load-shedding signal PMCU-4 issued 6 seconds after L3 tripped.

Fig. 8 shows a visual representation of power system dynamics obtained through use of EPG RTDMS software. Fig. 9 shows the same power system dynamics obtained through use of BPA PDC StreamReader software.

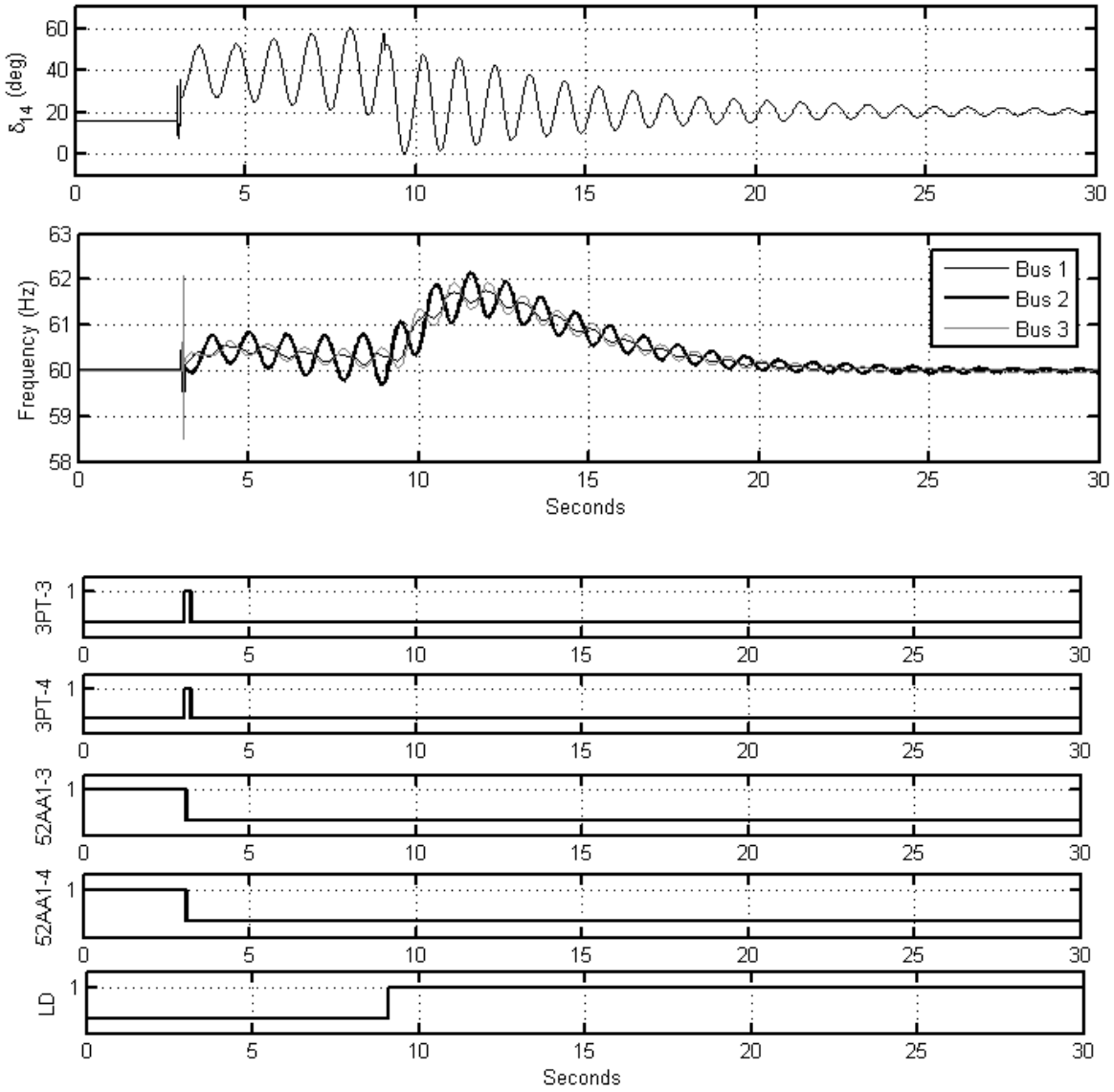

Fig. 7. RTDS event capture showing Bus 1-to-Bus 4 phase angle difference, frequency at Bus 1, Bus 2, and Bus 3, PMCU-3 and PMCU-4 trip commands, breaker status at both ends of line L3, and the load-shedding command.

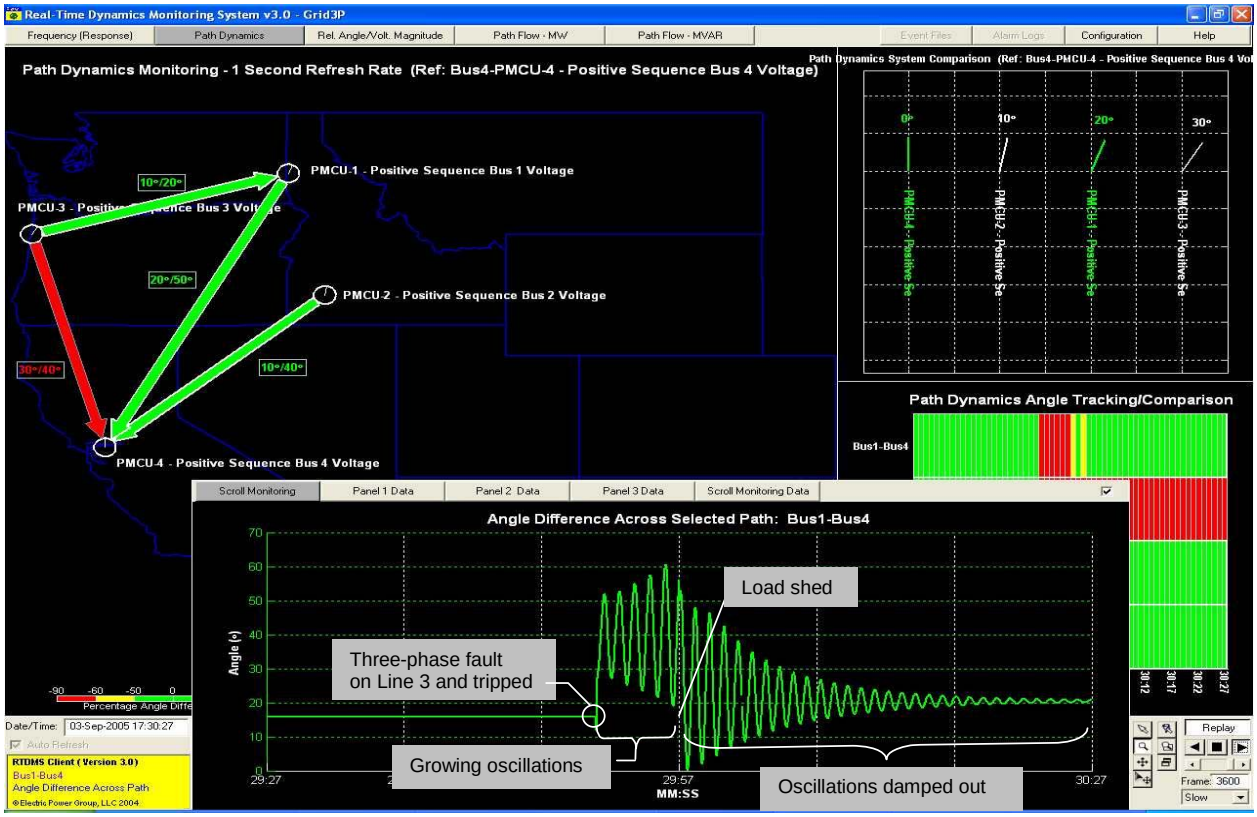

Fig. 8. EPG RTDMS capture for visualizing power system dynamics showing the phase angle difference between Bus 1 and Bus 4 for prefault, fault, and post-fault conditions. The system damped oscillations after load shedding.

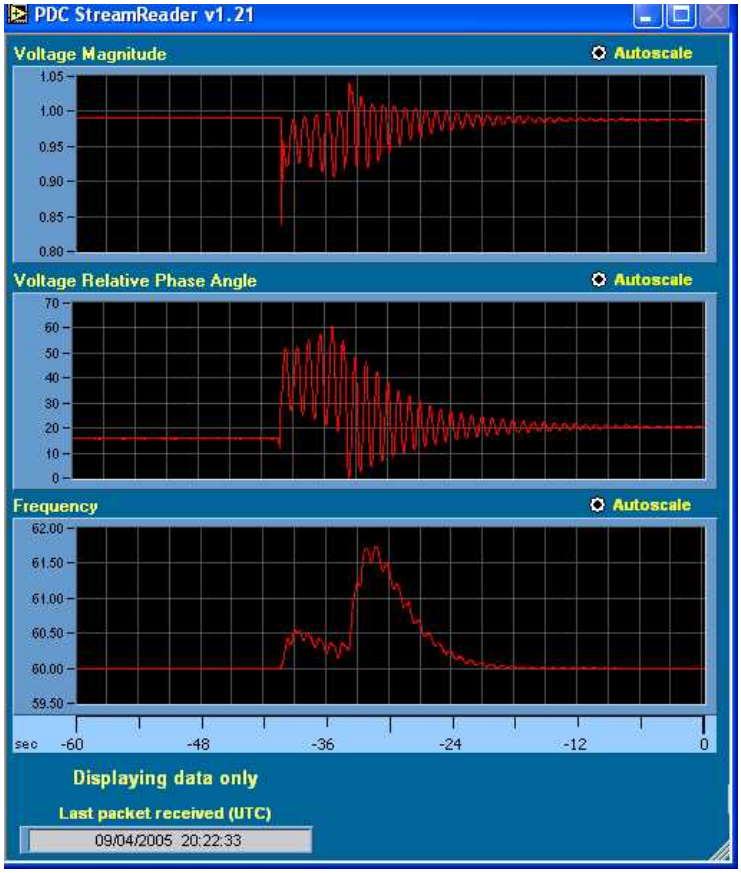

Fig. 9. BPA PDC StreamReader capture for visualizing power system dynamics showing Bus 1 voltage magnitude, Bus 1 to Bus 4 angle difference, and frequency at Bus 1.

3) Performance During Fault Conditions

Fig. 10 shows the positive-sequence impedance magnitude (normalized by the line impedance) that PMCU-3 measured for a three-phase fault at 50 percent of line L3. The measured positive-sequence impedance analog quantity is included with the synchrophasor data. Note that this impedance value is below the Zone 1 threshold (Z1TLC), indicating a Zone 1 fault. The second graph in Fig. 10 shows the A-phase synchrophasor voltage magnitude (set to per unit by the maximum value) measured at Bus 3. The third graph in Fig. 10 shows the synchrophasor data check. This check, which occurs after the synchrophasor data processor correlates data from PMCU-3 and PMCU-4, verifies that no synchrophasor data were lost during a fault condition. The check verifies that the time between one synchrophasor data packet and the next data packet is 1/60th of a 60 Hz cycle, an indicator of no lost data.

Fig. 11 shows the positive-sequence impedance magnitude PMCU-4 measured during the fault. The positive-sequence impedance analog quantity is included with the synchrophasor data. Note that this impedance value is below the Zone 1 threshold (Z1TRC) during the fault, indicating a Zone 1 fault. The second graph in Fig. 11 shows the A-phase synchrophasor voltage magnitude PMCU-4 measured at Bus 4. Notice that the voltage magnitude starts oscillating after L3 trips. The third graph in Fig. 11 shows that there was no loss of synchrophasor data during the fault condition. Fig. 12 shows the phase angle difference calculated from the correlated synchrophasor data measured by PMCU-3 and PMCU-4.

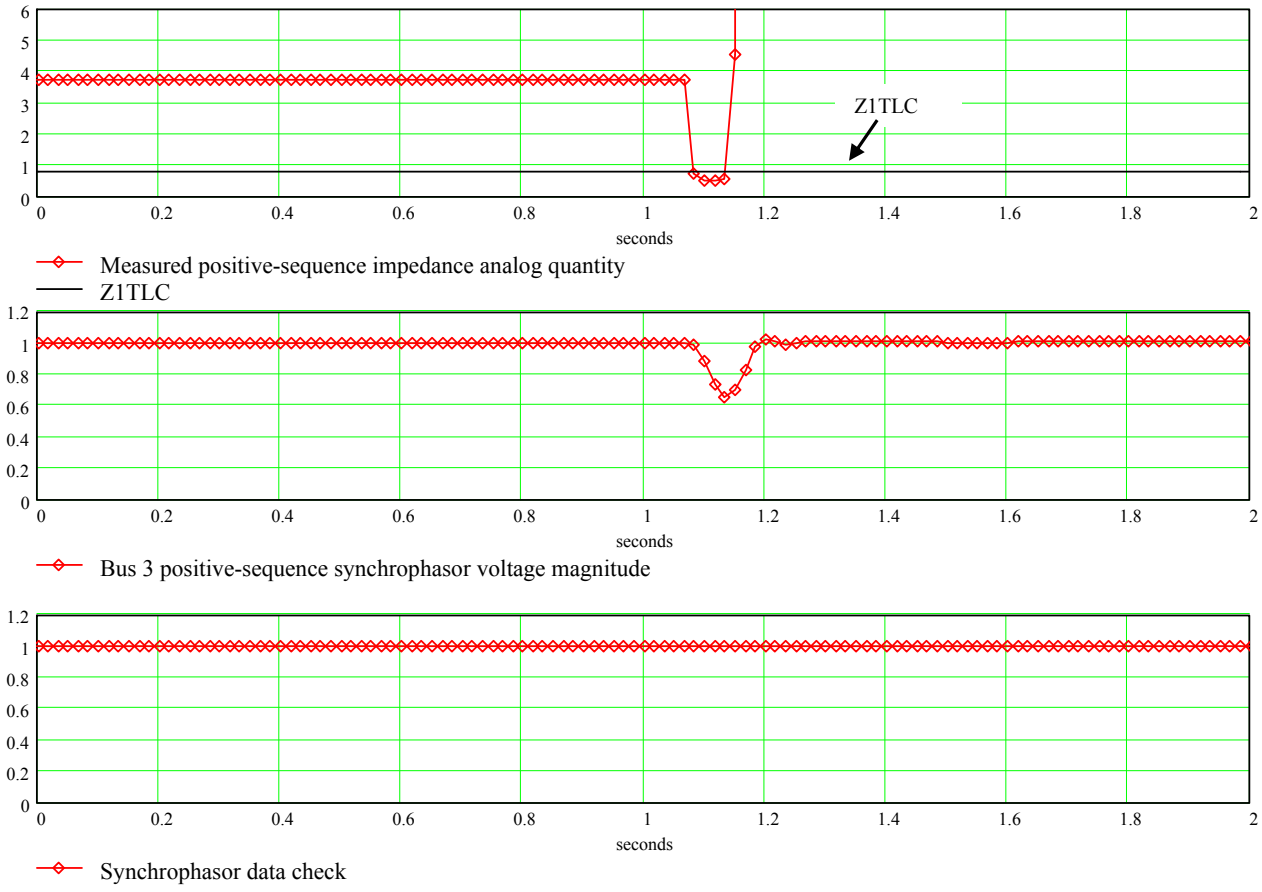

Fig. 10. Synchrophasor data (positive-sequence impedance and voltage magnitude) measured by PMCU-3 for a three-phase fault on L3. This figure also shows the synchrophasor data check for synchrophasor data loss.

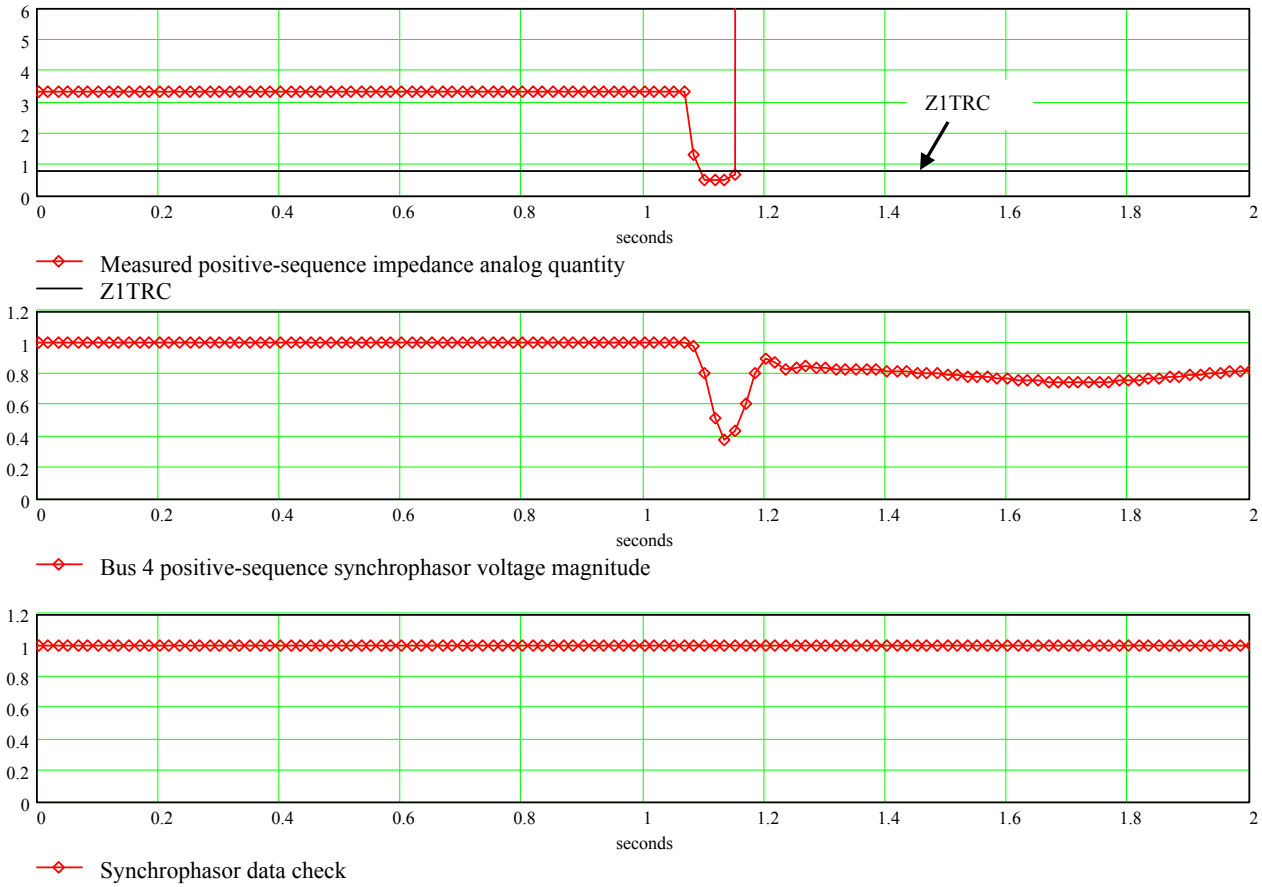

Fig. 11. Synchrophasor data (positive-sequence impedance and voltage magnitude) measured by PMCU-4 for a three-phase fault on L3. This figure also shows the synchrophasor data check for synchrophasor data loss.

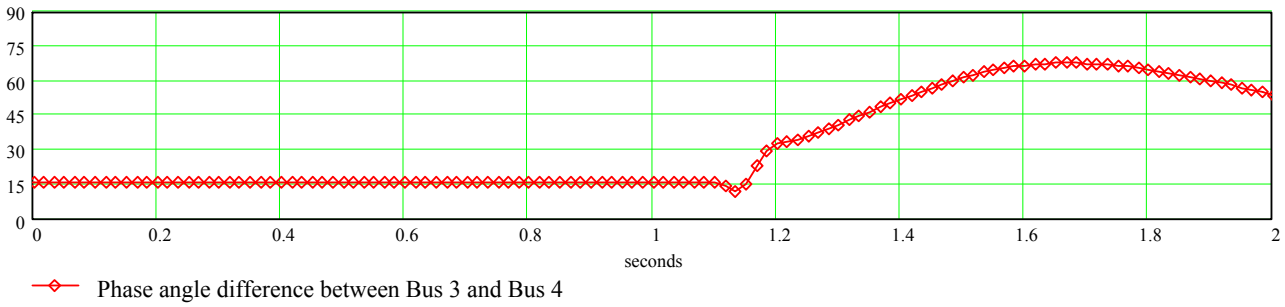

Fig. 12. Phase angle difference between Bus 3 and Bus 4 from the synchrophasor data measured by PMCU-3 and PMCU-4.

4) Two-Source Power System Model

The power system model in Fig. 13 consists of a 13.8 kV synchronous generator (G1) and a 230 kV infinite bus ② connected through a 13.8/230 kV step-up transformer (T1) and a transmission line (L1) as in [1]. The system parameters are given in Table II of Appendix A. For this model, we applied a three-phase fault at Bus 3 and cleared this fault at different times to demonstrate stable and unstable cases based on critical clearing time. Critical clearing time is the maximum time necessary to clear a fault so that the generator maintains a stable operating condition [6]. The critical clearing time for this case is 228 ms.

The model shows a synchronous generator with dynamics and excitation system. The mechanical power input to the machine is constant at 0.75 pu (i.e., there is no governor for speed control). The RTDS provides voltages and currents in real time and provides accurate representation of a real power system. PMCU-1 and PMCU-2 measure voltages at Bus 1 and Bus 2 and then synchronize and send the synchrophasor data to the synchrophasor data processor for visualization and archiving. The measured positive-sequence synchrophasor angle difference between PMCU-1 and PMCU-2 demonstrates dynamic response.

We applied a 100 ms three-phase fault at Bus 3. Fig. 14 shows the RTDS event capture. The first graph in Fig. 14 is the voltage phase angle difference between Bus 1 and Bus 2. The fault clears within the critical clearing time, so the generator returns to stable operation after oscillations damp out. The second graph shows the rotor angular velocity of the generator. The rotor angular velocity increases during the fault because the electrical power output is zero. Once the fault clears, the rotor begins oscillating and the generator returns to synchronism after the oscillations damp out. The third graph shows fault duration.

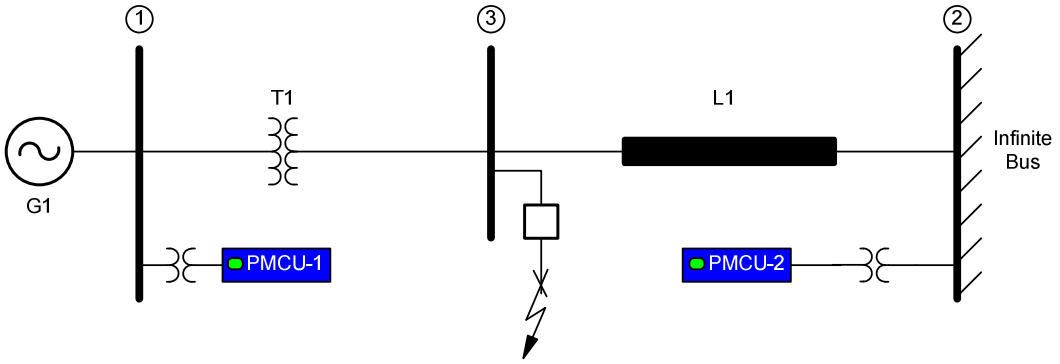

Fig. 13. Two-source RTDS power system model with two PMCUs for synchronized phasor measurement.

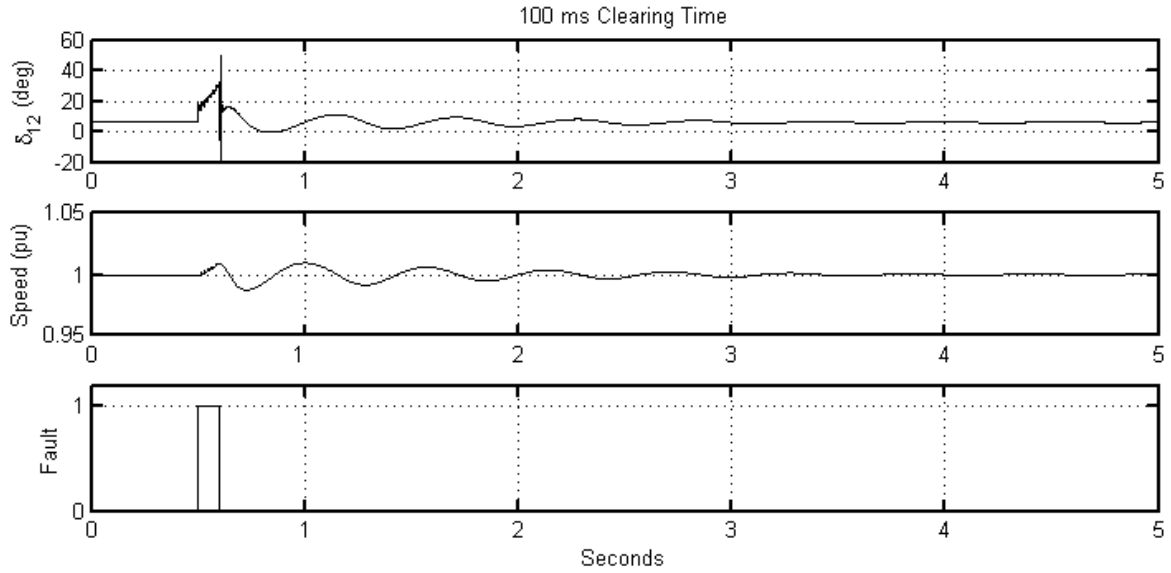

Fig. 14. RTDS event capture of phase angle difference (δ_{12}), rotor angular velocity (Speed), and fault duration (Fault) for a 100 ms three-phase fault.

Fig. 15 shows the synchrophasor voltage phase angle difference between Bus 1 and Bus 2 measured by PMCU-1 and PMCU-2 and δ_{12} from Fig. 14. The capture shows almost identical results from the measured PMCUs and the RTDS.

Fig. 16 shows the RTDS capture for a 200 ms three-phase fault at Bus 3. The fault clears within the critical clearing time, so the generator returns to stable operation after oscillations damp out. Note that in this case the generator needs more time than in the 100 ms case to damp out oscillations. The generator has gained more kinetic energy than for the 100 ms case, and so it needs more time to return energy back into the system.

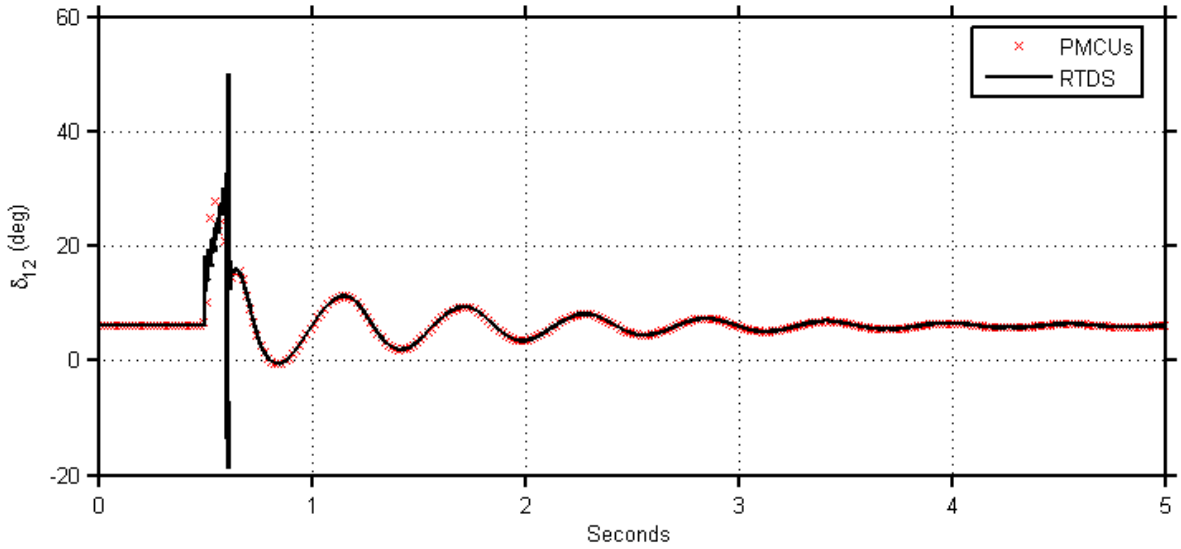

Fig. 15. Comparison of Bus 1 to Bus 2 phase angle difference measured by PMCUs and RTDS for a 100 ms three-phase fault.

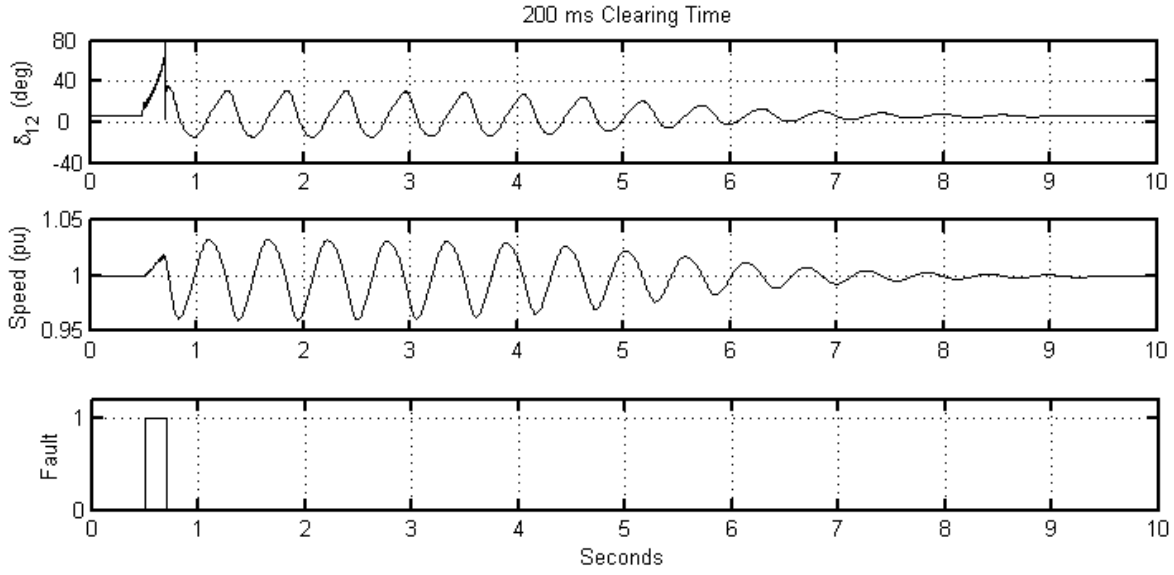

Fig. 16. RTDS event capture of phase angle difference (δ_{12}), rotor angular velocity (Speed), and fault duration (Fault) for a 200 ms three-phase fault.

Fig. 17 shows the synchrophasor voltage phase angle difference between Bus 1 and Bus 2 measured by PMCU-1 and PMCU-2 and δ_{12} from Fig. 16. The capture shows almost identical results from the measured PMCUs and the RTDS.

Fig. 18 shows the RTDS event capture for a 250 ms three-phase fault at Bus 3. The fault clears after the critical clearing time, but the generator becomes unstable. The rotor angular velocity increases beyond normal operating limits, which indicates that the generator lost synchronism with the infinite bus.

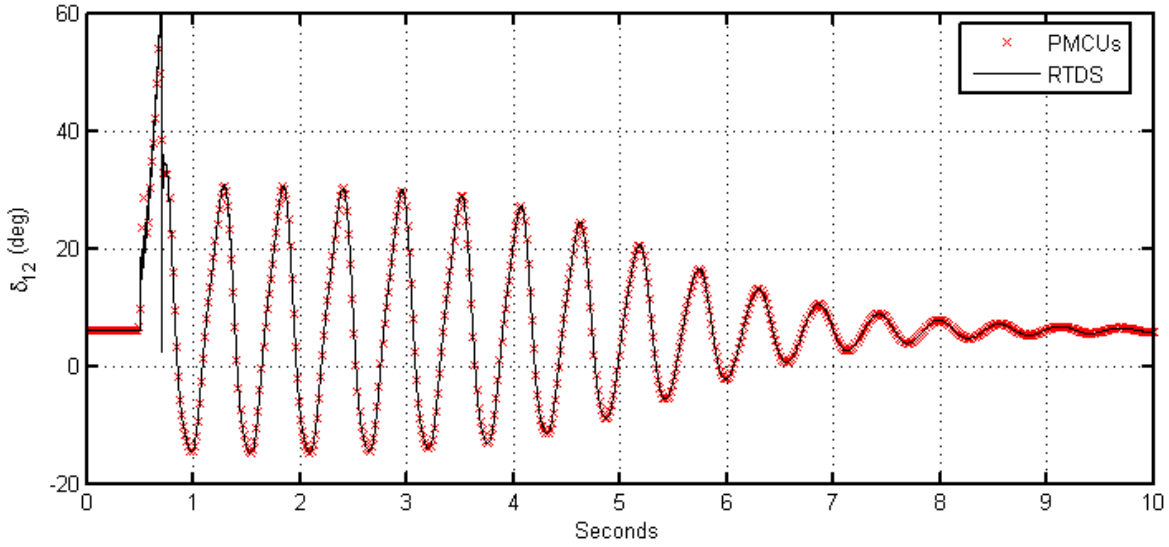

Fig. 17. Comparison of Bus 1 to Bus 2 phase angle difference measured by PMCUs and RTDS for a 200 ms three-phase fault.

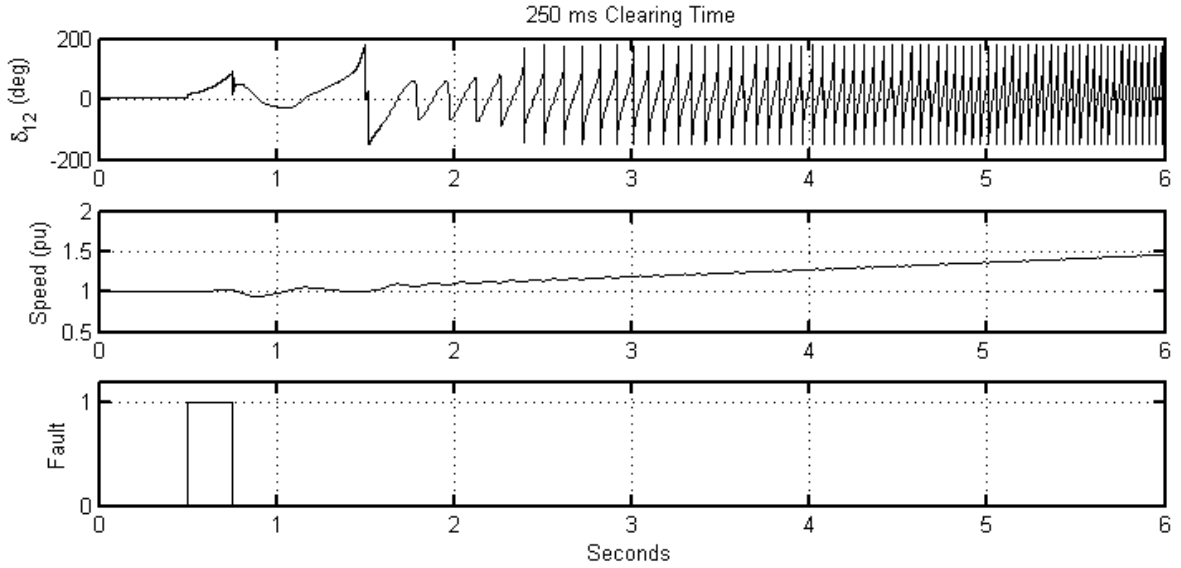

Fig. 18. RTDS event capture of phase angle difference (δ_{12}), rotor angular velocity (Speed), and fault duration (Fault) for a 250 ms three-phase fault.

Fig. 19 shows the synchrophasor voltage phase angle difference between Bus 1 and Bus 2 measured by PMCU-1 and PMCU-2 and δ_{12} from Fig. 18. Within the generator operating limits, the PMCU graph and the graph of the RTDS are identical. When the frequency is beyond the LPF cutoff frequency, the PMCU output is attenuated.

V. Conclusions

Synchronized phasor measurement devices require an absolute time reference for power system-wide applications. Traditional PMUs are expensive and not widely applied

Traditionally, numerical relays for line distance protection applications sample voltage and current signals at multiples of the operating power system frequency (f_{SYS}) to minimize phasor calculation errors. These relays have not been suitable for synchronized measurement applications.

This paper presents the method that a PMCU uses to acquire and process voltage and current signals for applications such as fault recording, synchronized phasor measurement, and line distance protection. The PMCU samples the signals at fixed time intervals with respect to an absolute time reference and resamples these signals at multiples of power system operating frequency. Synchronized phasor measurements use the sampled data with the absolute time reference. Distance protection uses filtered resampled data that minimize phasor calculation errors.

An adequate power system model during fault conditions demonstrates that the PMCU provides accurate synchrophasor calculations without interruption while performing protection functions. Thousands of PMCUs with the capabilities this paper describes have already been installed throughout North American power systems. Acquiring synchronized phasor measurements from these PMCUs is more economical than acquiring these measurements from traditional PMUs.

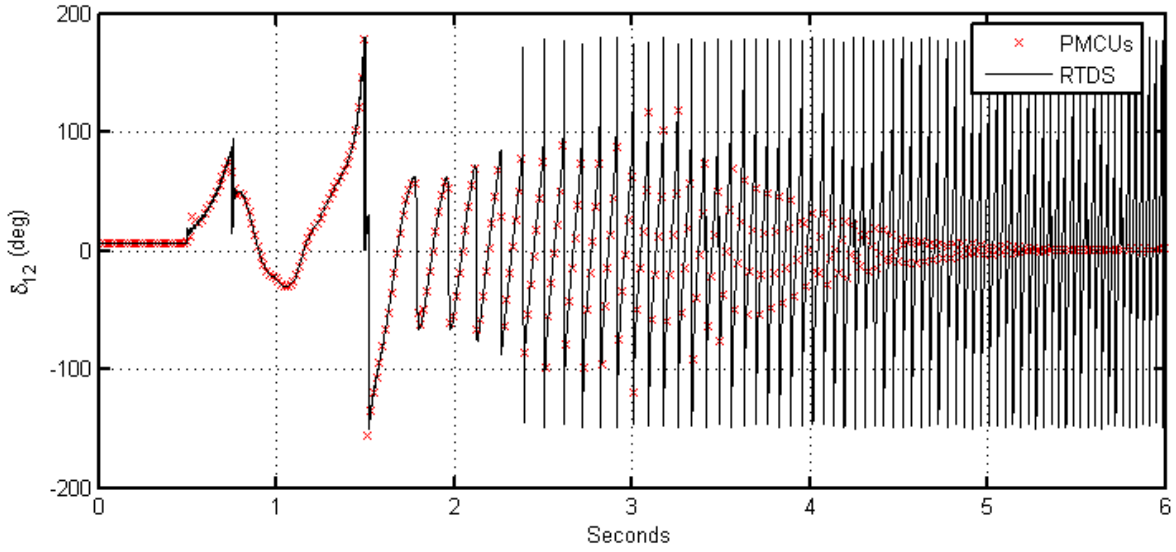

Fig. 19. Comparison of Bus 1 to Bus 2 phase angle difference measured by PMCUs and RTDS for a 250 ms three-phase fault.

VI. Appendix A

TABLE I
THREE-SOURCE RTDS® POWER SYSTEM MODEL DATA

Transmission line data	
Line Length	200 km
Positive-Sequence Line Impedance	98.11 ∠84.15º Ω
Zero-Sequence Line Impedance	255.99 ∠73.58º Ω
IEEE Type AC4 excitation	
Time Constant Tr (Tr)	0.0 s
Maximum Limit Vi Maximum (Vimx)	1.0 pu
Minimum Limit Vi Minimum (Vimn)	–1.0 pu
Lead Time Constant Tc (Tc)	1.0 s
Lag Time Constant Tb (Tb)	12 s
Gain Ka (Ka)	200
Time Constant Ta (Ta)	0.04 s
Maximum Limit Vr Maximum (Vrmx)	3 pu
Minimum Limit Vr Minimum (Vrmn)	0 pu
Constant Kc (Kc)	0.0
Hydroturbine Governor	
Generator Base Angular Frequency (HTZ)	60.0 Hz
Permanent Droop (PD)	0.0 pu
Temporary Droop (TD)	0.4 pu
Governor Time Constant (Tr)	5.0 s
Filter Time Constant (Tf)	0.035 s
Servo Time Constant (Tg)	0.05 s
Gate Velocity Limit (> 0.0) (VELM)	0.16 pu/s
Maximum Gate Position (< 1.0) (Gmax)	1.0 pu
Minimum Gate Position (≥ 0.0) (Gmin)	0.0 pu
Water Time Constant (Tw)	2.15 s
Turbine Gain (At)	1.27
Turbine Damping (Dt)	0.0
Generator Data	
Rated MVA	400 MVA
Inertia Constant (H)	3.0 MW • s/MVA
Load Data	
Type of Load	RL
Load Real Power	420 MW
Load Reactive Power	60 MVAr

TABLE II
TWO-SOURCE RTDS POWER SYSTEM MODEL DATA

Generator Data	
Rated MVA	200 MVA
Generator Transient Reactance	0.296 pu
Inertia Constant (H)	3.2 MW • s/MVA
Mechanical Power Input (Pm)	0.75 pu
Transformer Data	
Rated MVA	210 MVA
Transformer Reactance	0.152 pu
Transmission Line Data	
Positive-Sequence Line Impedance	17.61 ∠87.9º Ω
Zero-Sequence Line Impedance	80.14 ∠76º Ω

VII. Acknowledgment

The authors thank Dr. Manu Parashar from EPG and Ken Martin from BPA for providing visualization software tools.

VIII. References

[1] G. Benmouyal, E. O. Schweitzer, III and A. Guzmán, "Synchronized Phasor Measurement in Protective Relays for Protection, Control, and Analysis of Electric Power Systems," proceedings of the 29th Annual Western Protective Relay Conference, Spokane, WA, October 2002.

[2] E. O. Schweitzer, III and J. Roberts, "Distance Relay Element Design," proceedings of the 19th Annual Western Protective Relay Conference, Spokane, WA, October 1992.

[3] Working Group H-7, "Synchronized Sampling and Phasor Measurements for Relaying and Control," *IEEE Transactions on Power Delivery*, vol. 9, no. 1, pp. 442–452, January 1994.

[4] Ph. Denys, C. Counan, L. Hossenlopp, and C. Holweck, "Measurement of Voltage Phase for the French Future Defence Plan Against Losses of Synchronism," *IEEE Transactions on Power Delivery*, vol. 7, no. 1, pp. 62–69, January 1992.

[5] P. Kundur, *Power System Stability and Control*, New York: McGraw-Hill, 1994, p. 813.

[6] J. J. Grainger, W. D. Stevenson, *Power System Analysis*, New York: McGraw-Hill, 1994, p. 722.

IX. Biographies

Armando Guzmán received his BSEE with honors from Guadalajara Autonomous University (UAG), Mexico, in 1979. He received a diploma in fiber-optics engineering from Monterrey Institute of Technology and Advanced Studies (ITESM), Mexico, in 1990, and his MSEE from University of Idaho, USA, in 2002. He served as regional supervisor of the Protection Department in the Western Transmission Region of the Federal Electricity Commission (the electrical utility company of Mexico) in Guadalajara, Mexico for 13 years. He lectured at UAG in power system protection. Since 1993 he has been with Schweitzer Engineering Laboratories, Inc. in Pullman, Washington, where he is presently Research Engineering Manager. He holds several patents in power system protection and metering. He is a senior member of IEEE and has authored and coauthored several technical papers.

Satish Samineni received his B.E degree in electrical and electronics engineering from Andhra University College of Engineering, Visakhapatnam, India. He received his Master's degree in Electrical Engineering from University of Idaho, USA, in 2003. Since 2003, he has been with Schweitzer Engineering Laboratories, Inc. in Pullman, USA, where he presently holds the position of Power Engineer. His research interests include power electronics and drives, power system protection, synchrophasor-based control applications, and power system stability.

Mike Bryson received his BSEE from the University of Idaho in 1989. He joined Schweitzer Engineering Laboratories, Inc. as a Development Engineer in 1989. He has held the position of Power Engineer since 2001. His interests include development and testing of digital protection algorithms, signal processing, control systems, and real-time digital simulation of power systems.